Coding and non-coding transcriptome of mesial temporal lobe epilepsy

Critical role of small non-coding RNAs

Mills, J.D.; van Vliet, E.A.; Chen, B.J.; Janitz, M.; Anink, J.J.; Baayen, J.C.; Idema, S.; Devore, S.; Friedman, D.; Diehl, B.; Thom, M.; Scott, C.; Thijs, R.; Aronica, E.; Devinsky, O.

DOI
10.1016/j.nbd.2019.104612

Publication date
2020

Document Version
Final published version

Published in
Neurobiology of Disease

Neurobiology of Disease 134 (2020) 104612

Contents lists available at ScienceDirect

Neurobiology of Disease

journal homepage: www.elsevier.com/locate/ynbdi

Coding and non-coding transcriptome of mesial temporal lobe epilepsy: Critical role of small non-coding RNAs

James D. Mills[a,1], Erwin A. van Vliet[a,b,1], Bei Jun Chen[c], Michael Janitz[c], Jasper J. Anink[a], Johannes C. Baayen[d], Sander Idema[d], Sasha Devore[e], Daniel Friedman[e], Beate Diehl[f], Maria Thom[f], Catherine Scott[f], Roland Thijs[g], Eleonora Aronica[a,g,2], Orrin Devinsky[e,*,2]

[a] Amsterdam UMC, University of Amsterdam, Department of (Neuro)Pathology, Amsterdam Neuroscience, Meibergdreef 9, Amsterdam, the Netherlands
[b] Swammerdam Institute for Life Sciences, Center for Neuroscience, University of Amsterdam, Amsterdam, the Netherlands
[c] School of Biotechnology and Biomolecular Sciences, University of New South Wales, Sydney, New South Wales, Australia
[d] Amsterdam UMC, Vrije Universiteit Amsterdam, Department of Neurosurgery, Amsterdam Neuroscience, De Boelelaan 1117, Amsterdam, the Netherlands
[e] Comprehensive Epilepsy Center, New York University Langone Medical Center, New York, NY, USA
[f] Department of Clinical and Experimental Epilepsy, University College London Institute of Neurology, London, UK
[g] Stichting Epilepsie Instellingen Nederland (SEIN), Heemstede, the Netherlands

ARTICLE INFO

Keywords:
Epilepsy
Non-coding RNA
microRNA
Mesial temporal lobe epilepsy
Transcriptomics

ABSTRACT

Our understanding of mesial temporal lobe epilepsy (MTLE), one of the most common form of drug-resistant epilepsy in humans, is derived mainly from clinical, imaging, and physiological data from humans and animal models. High-throughput gene expression studies of human MTLE have the potential to uncover molecular changes underlying disease pathogenesis along with novel therapeutic targets. Using RNA- and small RNA-sequencing in parrallel, we explored differentially expressed genes in the hippocampus and cortex of MTLE patients who had undergone surgical resection and non-epileptic controls. We identified differentially expressed genes in the hippocampus of MTLE patients and differentially expressed small RNAs across both the cortex and hippocampus. We found significant enrichment for astrocytic and microglial genes among up-regulated genes, and down regulation of neuron specific genes in the hippocampus of MTLE patients. The transcriptome profile of the small RNAs reflected disease state more robustly than mRNAs, even across brain regions which show very little pathology. While mRNAs segregated predominately by brain region for MTLE and controls, small RNAs segregated by disease state. In particular, our data suggest that specific miRNAs (e.g., let-7b-3p and let-7c-3p) may be key regulators of multiple pathways related to MTLE pathology. Further, we report a strong association of other small RNA species with MTLE pathology. As such we have uncovered novel elements that may contribute to the establishment and progression of MTLE pathogenesis and that could be leveraged as therapeutic targets.

1. Introduction

Mesial temporal lobe epilepsy (MTLE), one of the most common forms of drug-resistant focal epilepsies, impairs quality-of-life, can progressively impair cognition and mental health, and can be fatal due to sudden death in epilepsy (SUDEP) or other causes (e.g., status epilepticus, accidents) (Bell et al., 2011; Devinsky et al., 2016). Hippocampal sclerosis is the most prevalent neuropathological finding in patients with drug-resistant MTLE and is characterized by neuronal loss, atrophy, inelasticity/hardness, and astroglial proliferation in the hippocampus (Blümcke et al., 2013; Thom, 2004). Surgical resection is a common treatment for MTLE patients, but complication can arise. Overall, surgery is effective in approximately 60% of cases, however, 25–35% of MTLE patients do not achieve sustained seizure freedom and some suffer cognitive and behavioral sequelae (Blumcke et al., 2017; Dredla et al., 2016; Engel et al., 2012; Kang et al., 2016; Pruitt et al., 2016). Moreover, many patients are not candidates for surgery. Thus, there is an urgent need to better understand the molecular mechanisms underlying MTLE to develop novel molecular-based therapies.

Previous transcriptional studies of hippocampal tissue from MTLE

* Corresponding author at: New York University Langone Medical Center, 223 E 34 Street, New York, NY 10016, USA.
E-mail address: od4@nyu.edu (O. Devinsky).
[1] these authors contributed equally to this work.
[2] these authors share senior authorship.

https://doi.org/10.1016/j.nbd.2019.104612
Received 31 July 2019; Received in revised form 21 August 2019; Accepted 6 September 2019
Available online 15 September 2019

patients identified profound changes in gene expression; however, these studies examined only one brain region, analyzed selective transcriptomic elements or were under-powered (Dixit et al., 2016; Griffin et al., 2016; Kaalund et al., 2014). Studies profiling differentially expressed mRNA and microRNAs (miRNAs) in animal MTLE studies are limited by heterogeneous seizure/epilepsy models and strains, leading to discordant results (Korotkov et al., 2017). Further, no study has analyzed other short non-coding RNAs elements of the transcriptome such as small nuclear RNAs or small nucleolar RNAs. These elements of the transcriptome represent important regulatory elements that are thought to play a critical role in cancer prognosis (Liao et al., 2010; Mei et al., 2012), but have not been studied in the context of MTLE. Performing RNA-Seq and small RNA-Seq on clinically well-characterized brain tissue resected during surgical treatment of drug-resistant MTLE patients offers a unique opportunity to assay all elements of the transcriptome towards developing a better understanding of the molecular mechanisms underlying the pathogenesis of MTLE.

In this study, we comprehensively analyzed all transcriptomic elements in parallel in fresh-frozen cortical and hippocampal tissue resected at surgery from MTLE patients using both RNA-Seq and small RNA-Seq. Using RNA-Seq we identified marked changes in the hippocampus of the MTLE patients when compared to controls but not in the cortex of MTLE patients. By contrast, small RNA-Seq revealed striking differences in the expression of miRNAs as well as other small non-coding RNAs in both the cortex and hippocampus of MTLE patients. Integration of the small RNA and mRNA transcriptomic profiles of the MTLE-HS identified 36 significantly enriched pathways that may be regulated by miRNAs, including many immune response and inflammation related pathways.

2. Materials and methods

2.1. Human tissue

The MTLE surgical tissue analyzed in this study was obtained from the archives of the departments of (Neuro)pathology of the Amsterdam University Medical Centers (Amsterdam UMC), the Netherlands, and University College London (UCL), United Kingdom. Informed consent was obtained from each Institutional Review Board (Amsterdam UMC and UCL) to use brain tissue and to access medical records. Tissue was used in accordance with the Declaration of Helsinki and the Amsterdam UMC Research Code provided by the Medical Ethics Committee and approved by the scientific committee of the university Biobank. For this study, 11 post-mortem control samples (5 cortical and 6 hippocampal) and 22 surgical MTLE samples (6 cortical and 16 hippocampal) were obtained. Table 1 summarizes the clinical characteristics of the patients and controls. All cases were reviewed independently by two neuropathologists and the classification of hippocampal sclerosis was based on International League Against Epilepsy criteria for microscopic examination (Blümcke et al., 2013). Control material was obtained during autopsy of age-matched individuals without a history of seizures or other neurological diseases.

2.2. RNA isolation

Frozen brain tissue was homogenized in Qiazol Lysis Reagent (Qiagen Benelux, Venlo, the Netherlands). Total RNA was isolated using the miRNeasy Mini kit (Qiagen Benelux, Venlo, The Netherlands) according to manufacturer's instructions. The concentration and purity of RNA was determined at 260/280 nm using a NanoDrop 2000 spectrophotometer (Thermo Fisher Scientific, Wilmington, DE, USA) and RNA quality was assessed using a Fragment Analyzer (Agilent technologies Netherlands, Amstelveen, the Netherlands).

Table 1
Samples used in this study.

Sample	Region	Gender	Epilepsy duration (years)	Age of onset (years)	Age (years)
MTLE-2	Cortex	Male	15	19	34
MTLE-3	Cortex	Male	9	21	29
MTLE-4	Cortex	Male	11	15	26
MTLE-5	Cortex	Female	23	9	32
MTLE-6	Cortex	Male	52	0	52
MTLE-7	Cortex	Male	15	7	22
MTLE-1	Hippocampus	Female	11	22	32
MTLE-3	Hippocampus	Male	9	21	29
MTLE-5	Hippocampus	Female	23	9	32
MTLE-6	Hippocampus	Male	52	0	52
MTLE-8	Hippocampus	Male	7	51	58
MTLE-9	Hippocampus	Male	30	3	33
MTLE-10	Hippocampus	Female	35	20	55
MTLE-11	Hippocampus	Female	42	1	43
MTLE-12	Hippocampus	Female	16	13	29
MTLE-13	Hippocampus	Female	17	15	32
MTLE-14	Hippocampus	Female	12	46	58
MTLE-15	Hippocampus	Female	22	23	45
MTLE-16	Hippocampus	Female	11	8	37
MTLE-17	Hippocampus	Female	50	14	64
MTLE-18	Hippocampus	Male	7	18	25
MTLE-19	Hippocampus	Male	8	17	25
Control-1	Cortex	Male	–	–	31
Control-4	Cortex	Male	–	–	31
Control-6	Cortex	Male	–	–	49
Control-7	Cortex	Male	–	–	57
Control-8	Cortex	Male	–	–	48
Control-1	Hippocampus	Male	–	–	31
Control-2	Hippocampus	Male	–	–	25
Control-3	Hippocampus	Female	–	–	44
Control-4	Hippocampus	Male	–	–	31
Control-5	Hippocampus	Male	–	–	75
Control-6	Hippocampus	Male	–	–	49

2.3. RNA-Seq library preparation and sequencing

All library preparation and sequencing were completed at GenomeScan (Leiden, the Netherlands). For RNA-Seq the NEBNext Ultra Directional RNA Library prep Kit for Illumina (New England Biolabs, Ipswich, MA, USA) was used in accordance with the manufacturer's protocols to process the samples and prepare the libraries for sequencing. In brief, ribosomal RNA (rRNA) was depleted from total RNA using a rRNA depletion kit (New England Biolabs, Ipswich, MA, USA). Next, RNA was fragmented and cDNA synthesis was performed. Sequencing adapters were ligated to the cDNA fragments followed by PCR amplification. Samples used for small RNA-Seq were processed using the TruSeq Small RNA-Seq preparation kit (Illumina, Foster City, CA, USA) in accordance with manufacturers' guidelines. Small RNA was isolated from purified RNA by size selection after ligation of sequencing adapters. After gel excision, the small RNA fragments were amplified by PCR. All clustering and DNA sequencing used the Illumina cBot and the HiSeq 4000. Both RNA-Seq and small RNA-Seq were subjected to paired-end sequencing with a read length of 151 nts to a depth of 50 million and 20 million reads, respectively.

2.4. Bioinformatics analysis of RNA-Seq data

Read quality was assessed using FastQC v0.11.2 software produced by the Babraham Institute (Babraham, Cambridgeshire, UK), and Trimmomatic v0.36 was used to filter reads of low quality (Bolger et al., 2014). Low quality leading and trailing bases were removed from each read, a sliding window trim using a window of 4 and a phred33 score threshold of 20 was used to assess the quality of the body of the read. We excluded any read < 75 nucleotides in length. Only reads with forward and reverse elements were included in downstream analysis.

Reads were aligned to the human reference genome, GRCh38 using TopHat2 v2.0.13 with the default settings (Kim et al., 2013). Using the featureCounts program from the Subread package, the number of reads that aligned to the genes in accordance with Gencode v27 were calculated (Harrow et al., 2012; Kozomara and Griffiths-Jones, 2014; Liao et al., 2014). Genes were only included in the differential expression analysis if they had ≥ 5 read counts in ≥ 4 samples. Differential expression was analyzed using the R package DESeq2 (Love et al., 2014). The false discovery rate was controlled for using the Benjamini-Hochberg correction, gene expression changes with an adjusted *p*-value < .05 were considered significant.

2.5. Bioinformatics analysis of small RNA-Seq data

Read quality was assessed using FastQC v0.11.2 software produced by the Babraham Institute (Babraham, Cambridgeshire, UK) and Trimmomatic v0.36 was used to filter reads of low quality (Bolger et al., 2014). Low quality leading and trailing bases were removed from each read, a sliding window trimming using a window of four and a phred33 score threshold of 15 was used to assess the quality of the read body. Any read < 17 nts was discarded. Both forward and reverse reads had to be present for reads to be included in downstream analysis.

Reads were aligned to the human reference genome, GRCh38 using Bowtie2 version 2.3.2 (Langmead and Salzberg, 2012), no mismatches between the seed sequence and the reference genome were allowed, reads were allowed to align a maximum of ten times. Using the featureCounts program from the Subread package the number of reads that aligned to the miRNAs, according to miRBase21 (Griffiths-Jones et al., 2008; Kozomara and Griffiths-Jones, 2014) (www.mirbase.org) and other short RNA species extracted from Gencode v27 were calculated (Harrow et al., 2012; Kozomara and Griffiths-Jones, 2014; Liao et al., 2014). Small RNAs with ≥ 5 read counts in ≥ 4 samples were considered expressed. Differential expression analysis was performed using the R package DESeq2 (Love et al., 2014). The false discovery rate was controlled for using the Benjamini-Hochberg correction, gene expression changes with an adjusted *p*-value < .05 were considered statistically significant.

2.6. Integrative bioinformatics

RNA-Seq and small RNA-Seq data were integrated using the R package “piano” (Väremo et al., 2013) and custom scripts written in R. The “piano” package is an open source tool available in R that can be used to perform gene set enrichment analysis (GSEA) using a variety of methods. The whole RNA transcriptome profile and the Reactome (Croft et al., 2011; Fabregat et al., 2018) gene to pathway dataset were fed to “piano”. The Wilcoxon rank-sum test method was used to identify enriched gene-sets among the dataset. Significance values were calculated through random gene sampling. First, a random set of genes equal in size to the gene-set being tested was selected and the gene set statistic was recalculated (Väremo et al., 2013). This was repeated 10,000 times to give a discrete null distribution. The gene set *p*-value was based on the fraction of random gene set statistics equal to or more extreme than the original gene set statistic. All *p*-values were corrected using the Benjamini-Hochberg method. Gene sets with an adjusted p-value < .05 were considered enriched. Next, gene sets enriched for differentially expressed genes were identified using Fisher's exact test. Gene sets with a Benjamini-Hochberg adjusted p-value < .05 were considered enriched for differentially expressed genes. Results were visualized using Cytoscape (Shannon et al., 2003).

Gene sets that were potentially modulated by miRNAs were then identified. First, the list of validated miRNA targets for each of the differentially expressed miRNAs was retrieved from miRWalk2 (Dweep et al., 2011; Dweep and Gretz, 2015). The validated miRNA targets from miRWalk2 are collected via an automated text-mining search, which is the collated with data from other databases. Each gene set that was enriched for differentially expressed genes was then assessed for over-representation of miRNA targets using Fisher's exact test. Gene sets with a Benjamini-Hochberg adjusted p-value < .05 were considered enriched for validated miRNA targets.

Finally, the expression levels of differentially expressed miRNAs and differentially expressed genes in the modules of interest were correlated to identify potentially miRNA-mRNA interaction partners. Correlations were calculated using Spearman's rank correlation, significant correlations (adjusted p-value < .05) of > 0.7 and less than −0.7 were deemed potential interesting interaction partners.

2.7. Quantitative reverse-transcription PCR analysis

To evaluate the gene expression of Cathepsin H (*CTSH*), matrix metallopeptidase 17 (*MMP17*), matrix metallopeptidase 14 (*MMP14*), and interleukain-1 beta (*IL1B*), 2.5 μg of total RNA was reverse-transcribed into cDNA using oligodT primers. PCR primers (Eurogentec, Belgium) were designed using the Universal ProbeLibrary of Roche (https://www.roche-applied-science.com) based on the reported cDNA sequences. The PCR master mix and data quantification was carried out in the same way as mentioned previously (Mills et al., 2017). The starting concentration of each product was divided by the starting concentration of the reference gene, eukaryotic translation elongation factor 1 alpha-1 (*eEF1A1*) and this ratio was compared between groups (Mann-Whitney *U* test); p-value < .05 was considered significant.

2.8. Connectivity map analysis

The connectivity map (CMap) uses cellular responses to perturbations to identify relationships between diseases and therapeutics (Subramanian et al., 2017). The top 150 up-regulated and top 150 down-regulated genes from MTLE-HS sorted by adjusted p-value were fed into CMap. These were then compared to the CMap database that contains over one million gene expression signatures that are derived from L1000 high-throughput assay to identify perturbagens that give an opposing gene signature to that entered.

3. Results

3.1. RNA-Sequencing of MTLE brain tissue

RNA-Seq was performed on total RNA extracted from 22 MTLE subjects obtained at surgery and 11 non-epileptic post-mortem control subjects. Each sample was sequenced to a depth of 50 million paired-end reads. After quality assessment and filtering ~48 million paired-end reads remained per sample of which ~84% mapped concordantly to the human reference genome GRCh38. Dimensionality reduction of the gene expression profile using the t-distributed stochastic neighbor embedding (t-SNE) machine learning algorithm and subsequent plotting identified three major clusters of samples (Fig. 1A). Cortical samples clustered together regardless of disease or control status, while MTLE hippocampal samples (MTLE-HS) and control hippocampal samples produced two distinct, divergent clusters.

Two differential gene expression analyses were carried out; control cortex was compared to MTLE cortex (MTLE-ctx) and control hippocampus was compared to MTLE-HS. In line with t-SNE clustering analysis, only two differential expressed genes were identified when the control cortex was compared to the MTLE-ctx – transcription factor 23 (*TCF23*) and the uncharacterized non-coding RNA *LOC101929719* (Fig. 1B). Both genes were up-regulated in the MTLE-ctx. On the other hand, when the control hippocampus was compared to the MTLE-HS, large perturbations to the transcriptome profile were identified; 2780 genes were up-regulated and 2952 were down-regulated (Fig. 1C). The top 10 up-regulated and down-regulated genes (ranked by adjusted *p*-value) are listed in Table 2. To validate the RNA-Seq data the genes *CTSH, IL1B MMP17* and *MMP14* were selected for analysis with RT-

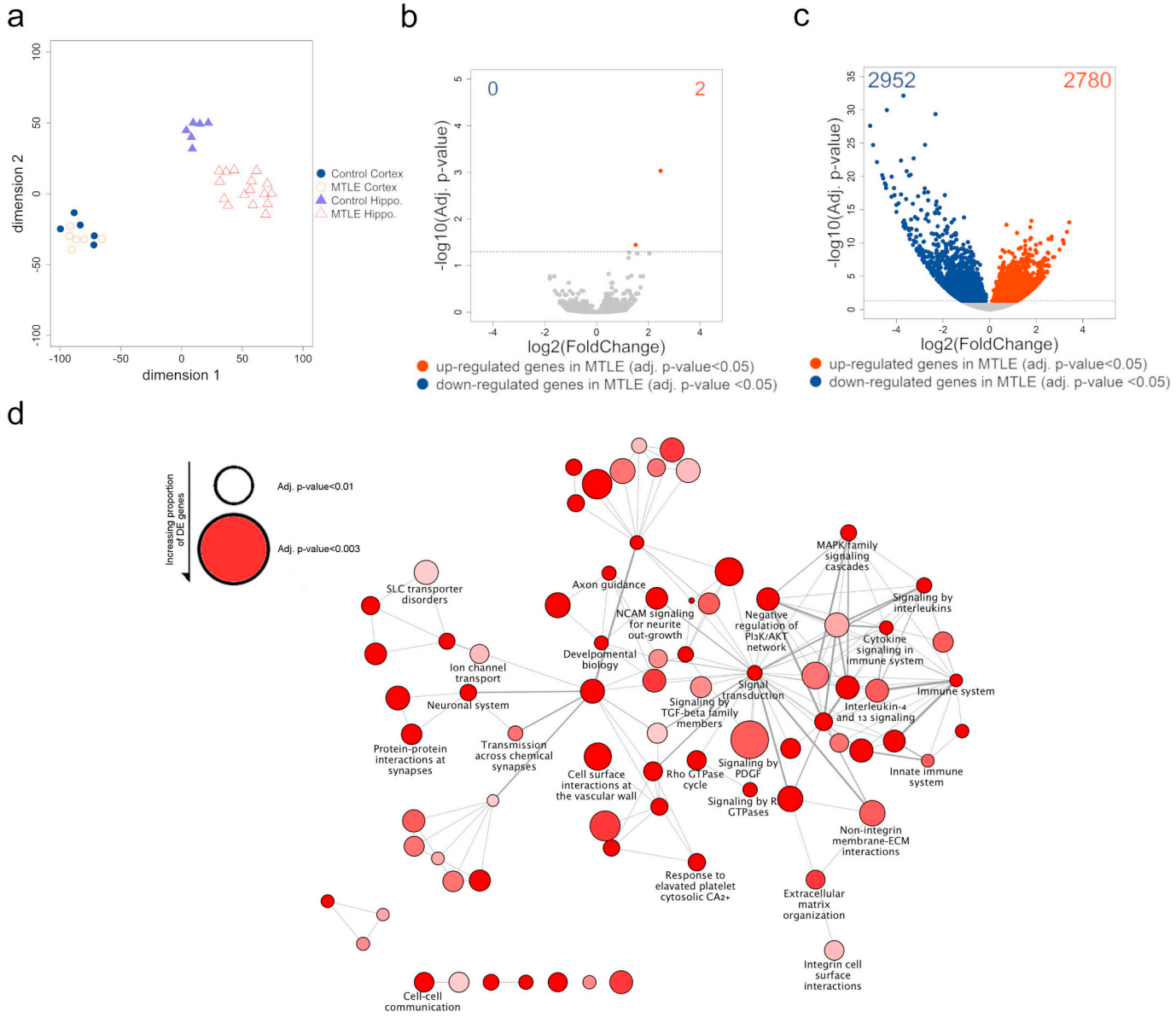

Fig. 1. RNA-Seq analysis of post-mortem tissue from cortex and hippocampus of mesial temporal lobe epilepsy cases. a. t-Distributed stochastic neighbor embedding (t-SNE) two-dimensional projection of the whole transcriptome profile generated from each sample. Each point represents a different sample. Samples from the cortex cluster together regardless of disease state. For the samples isolated from the hippocampus there was separation by disease state. b. Volcano plot showing differential expression of genes between MTLE cortex (n = 6) and control cortex (n = 5). Two genes were found to be up-regulated and no genes were down-regulated. Gene were considered differentially expressed if the adjusted p-value < .05. c. Volcano plot showing differential expression of genes between MTLE hippocampus (n = 6) and control hippocampus (n = 16). 2780 genes were found to be up-regulated and 2952 genes were down-regulated. Genes were considered differentially expressed if the adjusted p-value < .05. d. Visualisation of the significantly enriched pathways that were also enriched for the number of differentially expressed genes (adjusted p-value < .05). Here only pathways with an adjusted p-value < .01 are shown. Each node represents a different enriched pathway The size of node is proportional to the number of differentially expressed genes present in the pathway. The intensity of the node colour indicates the adjusted p-value, with white indicating an adjusted p-value < 0.01 and red indicating a p-value < 0.03. Edges between nodes indicates shared genes in the pathway.

qPCR (Supp. Fig. 1). In line with the RNA-Seq data the genes *CTSH* and *IL1B* were significantly up-regulated (Mann-Whitney-U; p-value < .05) and *MMP14* was significantly down-regulated (Mann-Whitney-U; p-value < .05). While *MMP17* appeared to be down-regulated, the change was not statistically significant.

A gene set enrichment analysis (GSEA) (see methods) was performed on the transcriptome profile generated from the RNA-Seq analysis of the control and MTLE-HS samples. 150 distinct pathways were significantly enriched (adjusted p-value < .05) and were also enriched for differentially expressed genes (Fisher's exact test, adjusted p-value < .05) (Supp. Table 1). The hippocampal transcriptome profile was enriched for pathways that included the immune system and immune cytokine signaling, MAPK family signaling cascades and negative regulation of the PI3K/AKT network (Fig. 1D).

To delineate the potential cell-types perturbed in MTLE-HS pathology, we analyzed an independent dataset of single-cell RNA-Seq from neurons, microglia, oligodendrocytes and astrocytes taken from the healthy human brain (GSE67835) (Darmanis et al., 2015). Genes from the single-cell RNA-Seq analysis were classified as microglia, oligodendrocyte, astrocyte and neuron specific based on expression values (> 10 read-counts in cell type of interest, < 1 read count in all other cell-types). Of the 2780 genes up-regulated in MTLE-HS, 21 were specific to astrocytes, 9 to oligodendrocytes, 12 to neurons, and 41 to microglia (Supp. Table 2). Among the 2952 down-regulated genes in

Table 2
Top 10 up-regulated and down-regulated genes in the MTLE hippocampus sorted by adjusted p-value.

Top 10 over-expressed genes in MTLE-HS

Gene	Description	Chr. Location	Log2(FC)	Adj. p-value
TAL1	TAL bHLH transcription factor 1, erythroid differentiation factor	chr1:47216290–47,232,220	1.89	4.81E-14
CCL3	C-C motif chemokine ligand 3	chr17:36088256–36,090,169	4.50	7.78E-14
SEMA6D	Semaphorin 6D	chr15:47184101–47,774,223	0.74	1.91E-13
GGTA1P	Glycoprotein, alpha-galactosyltransferase 1 pseudogene	chr9:121444991–121,500,027	1.83	4.27E-13
TNF	Tumor necrosis factor	chr6:31575567–31,578,336	4.62	2.17E-12
FMNL3	Formin like 3	chr12:49636499–49,708,165	1.20	3.10E-12
CH25H	Cholesterol 25-hydroxylase	chr10:89205629–89,207,314	3.16	1.15E-11
OGFRL1	Opioid growth factor receptor like 1	chr6:71288803–71,308,950	1.87	1.72E-11
AC245014.3	Long intergenic non-coding RNA	chr1:145281116–145,281,462	2.89	2.60E-11
EGR2	Early growth response 2	chr10:62811996–62,919,900	3.14	2.78E-11

Top 10 under-expressed genes in MTLE-HS

Gene	Description	Chr. Location	Log2(FC)	Adj. p-value
TTR	Transthyretin	chr18:31591726–31,591,726	−11.22	3.28E-55
PRLR	Prolactin receptor	chr5:35048756–35,230,589	−8.07	2.41E-51
FOLR1	Folate receptor 1	chr11:72189558–72,196,323	−8.59	7.68E-33
DNAH11	Dynein axonemal heavy chain 11	chr7:21543215–21,901,839	−4.24	7.68E-33
SERPINF1	Serpin family F member 1	chr17:1761959–1,777,574	−5.37	1.14E-30
SERPIND1	Serpin Family D Member	chr22:20707686–20,891,218	−2.45	4.52E-30
SLC13A4	Solute Carrier Family 13 Member 4	chr7:135662487–135,748,846	−7.40	2.53E-28
SLC5A5	Solute Carrier Family 5 Member 5	chr19:17871961–17,895,174	−3.05	1.87E-25
DCX	Doublecortin	chrX:111293779–111,412,375	−8.13	1.93E-25
ST8SIA2	ST8 alpha-*N*-acetyl-neuraminide alpha-2,8-sialyltransferase 2	chr15:92393827–92,468,728	−3.75	2.00E-23

MTLE-HS, 41 were specific to neurons, 12 to astrocytes, 7 to microglia and 6 to oligodendrocytes (Supp. Table 2). Hypergeometric testing revealed that genes up-regulated in the hippocampus were significantly enriched for astrocytes ($p < .01$) and microglia ($p < .01$), while the down-regulated genes were significantly enriched for neurons ($p < .01$).

3.2. Small RNA-Sequencing of MTLE brain tissue

Small RNA-Seq was performed on the same samples analyzed for RNA-Seq. Each sample was sequenced to a depth of ~20 million reads. After quality assessment and filtering, ~16 million reads remained, of which 88% were successfully mapped to the human reference genome GRCh38. Dimensionality reduction of the gene expression profile using the t-SNE algorithm and subsequent plotting identified two major clusters (Fig. 2A). Interestingly, whereas the standard RNA-Seq was reflective of brain region, the small RNA-Seq profiles reflected disease state, with both the MTLE-ctx and MTLE-HS clustering distinctly from the control cortex and hippocampus. This suggests that small RNAs reflect disease state more accurately than the mRNA fraction and are able to distinguish MTLE pathogenesis more readily from the control state.

In contrast to the standard RNA-Seq, small RNAs were identified as differentially expressed when the MTLE-ctx was compared to the control cortex. Overall, there were 66 small RNAs that were up-regulated and 142 down-regulated small RNAs (Fig. 2B). The top 10 up-regulated and down-regulated small RNAs (ranked by adjusted *p*-value) are listed in Table 3. When MTLE-HS was compared to control hippocampus there were 218 up-regulated and 448 were down-regulated small RNAs (Fig. 2C). Next, the biotypes of the differentially expressed small RNAs were assessed, the most common biotype of differentially expressed small RNAs in both the MTLE-HS and MTLE-ctx was small nuclear RNAs, followed by miRNAs (Fig. 2D-E). Finally, the overlap of miRNAs and other small non-coding RNAs from hippocampus and cortex were analyzed (Supp. Fig. 2). Of the differentially expressed miRNAs in the MTLE-HS, only 9% of up-regulated miRNAs and 16% of down-regulated miRNAs were also differentially expressed in the MTLE cortex. By contrast, among other small RNA species, 44% of those up-regulated and 32% of those down-regulated in the MTLE-HS were similarly up- or down-regulated in the MTLE-ctx. This result suggests that the expression patterns of the other small non-coding RNAs, including snoRNAs and snRNAs, are more conserved across brain regions of patients with MTLE than the expression changes of miRNAs or mRNAs.

3.3. Bioinformatic integration of small RNA-Sequencing and RNA-Sequencing data

To identify key miRNAs that may regulate pathogenic or altered pathways in the hippocampus of MTLE patients, each of the 150 enriched pathways from the GSEA were assessed for over-representation of validated miRNA targets of the differentially expressed miRNAs. Of the enriched pathways, 36 were enriched for validated miRNA targets (Fisher' s Exact test, adjusted p-value < .05) (Fig. 3).

Next, we analyzed individual correlations between miRNAs and their validated gene targets within each pathway to identify potentially important miRNA-mRNA pairs. Among the miRNAs of interest, let-7b-3p and let-7c-3p had the greatest number of correlations with differentially expressed genes '− . Expression of let-7b-3p was negatively correlated with five differentially expressed genes (Spearman's rank correlation < −0.7, adjusted p-value < .05) and positively correlated with eight differentially expressed genes (Spearman's rank correlation > 0.7, adjusted p-value < .05) (Supp. Table 3). Let-7c-3p was negatively correlated with ten differentially expressed genes (Spearman's rank correlation < −0.7, adjusted p-value < .05) and positively correlated with 20 differentially expressed genes (Spearman's rank correlation > 0.7, adjusted p-value < .05) (Supp. Table 3). Furthermore, let-7b-3p and let-7c-3p, were predicted as major regulators of 15 and 19 different pathways, respectively, of which 12 pathways were common to both miRNAs. Of particular interest were the negative correlations between let-7b-3p and Trio Rho Guanine Nucleotide Exchange Factor (*TRIO*) and Prostaglandin E Synthase 2 (*PTGES2*), and let-7c-3p and DEAD-Box Helicase 41 (*DDX41*), SWI/SNF Related Matrix Associated, Actin Dependent Regulator of Chromatin, Subfamily A, Member 4 (*SMARCA4*) and Lysine Methyltransferase 2D (*KMT2D*) (Fig. 4). Each of

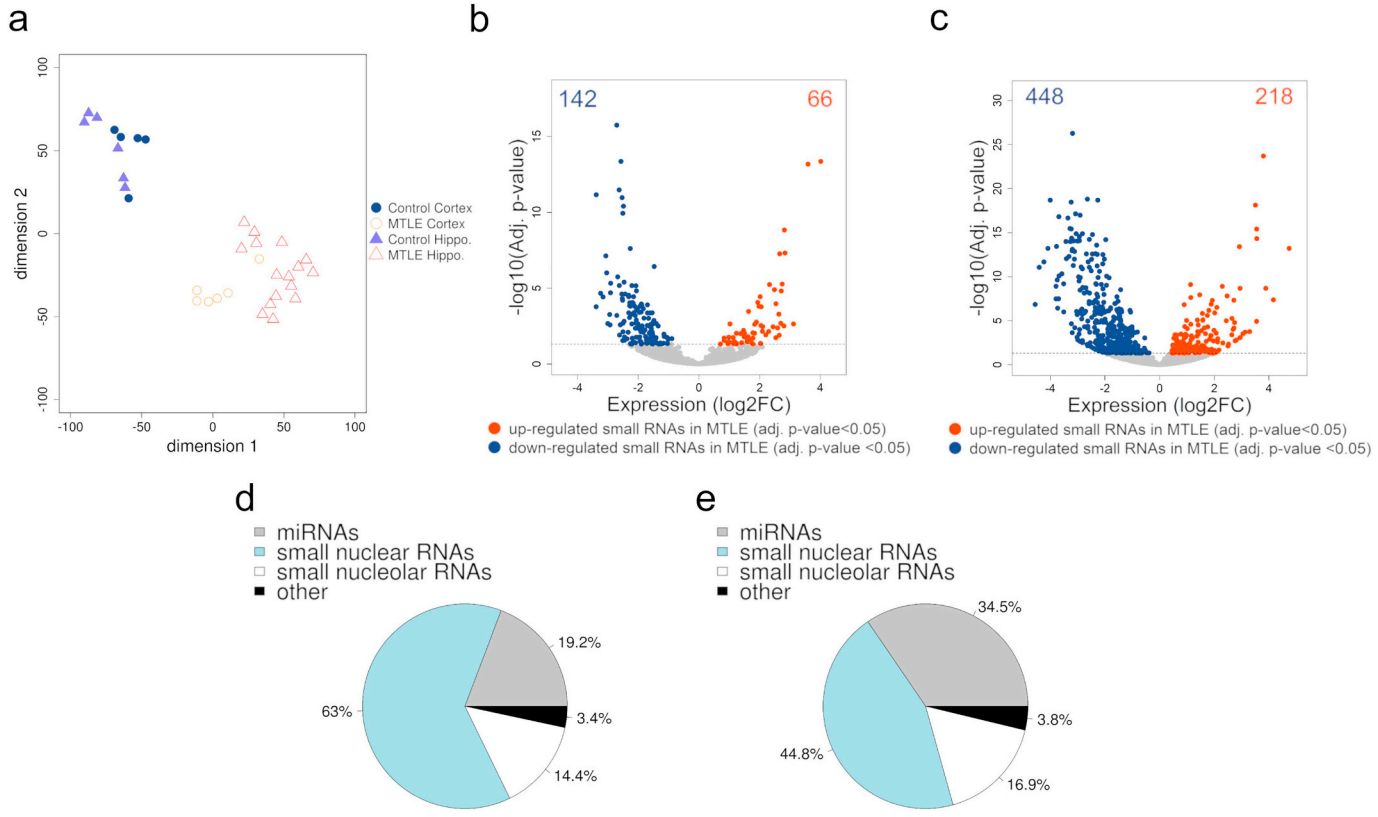

Fig. 2. Small RNA-Seq analysis of post-mortem tissue from cortex and hippocampus of mesial temporal lobe epilepsy cases. a. t-SNE two-dimensional projection of the small RNA expression profile generated from each sample. Each point represents a different sample. In contrast to the RNA-Seq data samples cluster by disease state rather than brain region. b. Volcano plot showing differential expression of small RNAs between MTLE hippocampus (n = 6) and control hippocampus (n = 16). 66 small RNAs were found to be up-regulated and 142 small RNAs were down-regulated. Small RNAs were considered differentially expressed if the adjusted *p*-value < .05. c. Volcano plot showing differential expression of small RNAs between MTLE hippocampus (n = 6) and control hippocampus (n = 16). 218 small RNAs were found to be up-regulated and 448 small RNAs were down-regulated. Small RNAs were considered differentially expressed if the adjusted p-value < .05. d. Biotypes of differentially expressed small RNAs in the cortex. Small nuclear RNAs made up the majority of the differentially expressed small RNAs, followed by small nucleolar RNAs, and miRNAs. e. Biotypes of differentially expressed small RNAs in hippocampus. Small nuclear RNAs made up the majority of the differentially expressed small RNAs, followed by small nucleolar RNAs, and miRNAs.

these genes were present in the inflammation and immune response related enriched pathways.

3.4. Connectivity map analysis

The up-regulated and down-regulated gene lists from the MTLE-HS were analyzed using the connectivity map (CMap) (see methods) to identify compounds that would give rise to a gene signature that opposes the gene signature observed in MTLE-HS. The top five compounds identified included dictamnine, which has diverse biological activities, such as antifungal, antibacterial, vascular-relaxing, antiplatelet aggregation, anti-hypertension and anti-tumor activities, the MEK inhibitor PD-0325901, the MTOR inhibitor deforolimus, the anti-inflammatory compound celastrol, and the estrogen receptor agonist dairylpropionitrile. These compounds are already approved for use in humans and as such could be repurposed for use in the treatment of MTLE.

4. Discussion

We found striking differences in the RNA and small RNA transcriptome profiles in the hippocampus of patients with MTLE compared to control hippocampus. The RNA transcriptome from MTLE patients showed 2780 up-regulated genes and 2952 down-regulated genes compared to controls. We identified an enrichment of 150 pathways within the transcriptome profile of the MTLE hippocampus, including immune function, cytokine signaling, MAPK signaling and PI3K/AKT network. In contrast, the cortical expression patterns were similar among patients and controls with only two genes up-regulated in MTLE. Interestingly, there were marked differences in small RNA expression in both the cortex and hippocampus of MTLE patients compared to controls. In the MTLE-ctx, 66 small RNAs were up-regulated and 142 were down-regulated. In the MTLE-HS, 218 small RNAs were up-regulated and 448 were down-regulated. Integration of the small RNA and RNA transcriptome profiles of the MTLE-HS identified 36 significantly enriched pathways that may be regulated by miRNAs, including many immune response and inflammation related pathways.

We observed distinct differences between the clustering of the RNA and the small RNA transcription profiles. While RNAs could be used to clearly define the brain region from which the sample was extracted, the small RNA transcriptome profile clustered by disease state, entirely independent of brain region. For both the MTLE-ctx and the MTLE-HS the most common biotype of differentially expressed small RNAs was small nuclear RNAs, followed by miRNAs and then small nucleolar RNAs. Interestingly, expression changes in the other small non-coding RNA species were relatively more conserved between the hippocampus and cortex when compared to miRNAs, which showed greater regional divergence. These findings suggest that small non-coding RNAs may be involved in the initial underlying molecular pathogenesis of MTLE, or the brain's compensatory changes to suppress epileptogenesis and seizures. While small nucleolar RNAs have been implicated in cancer (Liao et al., 2014; Mei et al., 2012) and small nuclear RNAs in Alzheimer's

Table 3
Top 10 up-regulated and down-regulated small RNA in the MTLE cortex and hippocampus sorted by adjusted p-value.

Cortex				
Top 10 over-expressed small non-coding RNAs				
Gene	Class	Chr. Location	Log2(FC)	Adj. p-value
RNU6-576P	Small nuclear RNA, pseudogene	chr1:47216290–47,232,220	4.02	4.48E-14
RNU6-211P	Small nuclear RNA, pseudogene	chr17:36088256–36,090,169	3.59	6.68E-14
RNU6-1133P	Small nuclear RNA, pseudogene	chr15:47184101–47,774,223	2.82	1.48E-09
RNU6-1141P	Small nuclear RNA, pseudogene	chr9:121444991–121,500,027	2.84	4.83E-08
hsa-miR-4443	microRNA	chr6:31575567–31,578,336	2.66	5.46E-08
RNU6-735P	Small nuclear RNA, pseudogene	chr12:49636499–49,708,165	2.74	5.39E-06
RNU6-61P	Small nuclear RNA, pseudogene	chr10:89205629–89,207,314	2.32	5.77E-06
RNU6-673P	Small nuclear RNA, pseudogene	chr6:71288803–71,308,950	2.49	1.26E-05
RNU6-1187P	Small nuclear RNA, pseudogene	chr1:145281116–145,281,462	2.72	1.52E-05
RNU6-256P	Small nuclear RNA, pseudogene	chr10:62811996–62,919,900	2.02	3.68E-05
Top 10 under-expressed genes small non-coding RNAs				
Gene	Class	Chr. Location	Log2(FC)	Adj. p-value
hsa-miR-320d	microRNA	chr18:31591726–31,591,726	−2.71	1.81E-16
hsa-miR-320e	microRNA	chr5:35048756–35,230,589	−2.57	4.48E-14
RNU4-91P	Small nuclear RNA, pseudogene	chr11:72189558–72,196,323	−2.63	3.38E-12
RNU4-30P	Small nuclear RNA, pseudogene	chr7:21543215–21,901,839	−3.39	6.98E-12
RNU4-6P	Small nuclear RNA, pseudogene	chr17:1761959–1,777,574	−2.53	1.08E-11
RNU4-82P	Small nuclear RNA, pseudogene	chr22:20707686–20,891,218	−2.49	4.00E-11
U4	Small nuclear RNA	chr7:135662487–135,748,846	−2.51	1.16E-10
SNORD38	Small nucleolar RNA	chr19:17871961–17,895,174	−2.27	2.44E-08
RNU4-53P	Small nuclear RNA, pseudogene	chrX:111293779–111,412,375	−3.07	7.51E-08
hsa-miR-320c	microRNA	chr15:92393827–92,468,728	−1.48	3.77E-07
Hippocampus				
Top 10 over-expressed small non-coding RNAs				
Gene	Class	Chr. Location	Log2(FC)	Adj. p-value
hsa-miR-4443	microRNA	chr3:48196564–48,196,616	3.80	2.05E-24
RNU6-1141P	Small nuclear RNA, pseudogene	chr10:21661635–21,661,741	3.51	7.68E-19
RNU6-576P	Small nuclear RNA, pseudogene	chr10:2199387–2,199,488	3.55	4.01E-16
RNU6-735P	Small nuclear RNA, pseudogene	chr12:95438737–95,438,843	3.56	4.79E-15
RNU6-211P	Small nuclear RNA, pseudogene	chr5:80365726–80,365,832	2.92	3.92E-14
hsa-miR-4455	microRNA	chr4:184938383–184,938,440	4.74	6.20E-14
hsa-let-7c-3p	microRNA	chr21: 16539828–16,539,911	1.13	7.93E-10
RNU6-61P	Small nuclear RNA, pseudogene	chr13:8069426–80,369,534	2.230	1.26E-09
RNU6-1327P	Small nuclear RNA, pseudogene	chr9:558826–558,930	2.94	2.09E-09
RNU7-26P	Small nuclear RNA, pseudogene	chr6:27897504–27,897,566	3.89	2.10E-09
Top 10 under-expressed genes small non-coding RNAs				
Gene	Class	Chr. Location	Log2(FC)	Adj. p-value
hsa-miR-1298-5p	microRNA	chrX: 114715233–114,715,344	−6.54	1.03E-43
hsa-miR-1911-5p	microRNA	chrX: 114763184–114,763,263	−7.57	1.39E-43
SNORD38	Small nucleolar RNA	chr19:3521248–3,521,320	−3.19	5.31E-27
SNORA44	Small nucleolar RNA	chr1:28580381–28,580,512	−2.64	1.58E-19
SNORA6	Small nucleolar RNA	chr3:39408389–39,408,539	−4.00	2.09E-19
hsa-miR-320d	microRNA	chr13: 40727816–40,727,887,	−2.26	2.09E-19
RNU6-140P	Small nuclear RNA, pseudogene	chr19:38797002–38,797,109	−3.24	3.50E-19
RNU6-443P	Small nuclear RNA, pseudogene	chr1:13279125–13,279,231	−3.08	7.37E-18
RNU6-164P	Small nuclear RNA, pseudogene	chr5:162477891–162,477,993	−2.91	1.06E-17
hsa-miR-204-5p	microRNA	chr9: 70809975–70,810,084	−3.69	1.58E-17

disease (Bai et al., 2013) these elements have never been investigated in terms of MTLE. The results presented here suggest that these understudied elements of the transcriptome require more attention for disease modifying roles in MTLE. Further studies to determine whether these changes are part of the pathology or compensatory changes in MTLE could result in the development of new therapeutic tools.

In the present study, let-7b-3p and let-7c-3p were predicted as regulators of 15 and 19 different enriched pathways respectively. This suggests that these miRNAs may act as critical regulators of the MTLE transcriptional networks. miRNAs from the lethal-7 (let-7) family were among the first miRNAs to be discovered and are evolutionarily conserved across various animal species (Lee et al., 2016). Previously, let-7b was shown to regulate cell proliferation and differentiation in the cortex of mice during development (Zhao et al., 2010). Knock-down of let-7b resulted in enhanced proliferation of neural stem cells, while over-expression of let-7b decreases proliferation and accelerates

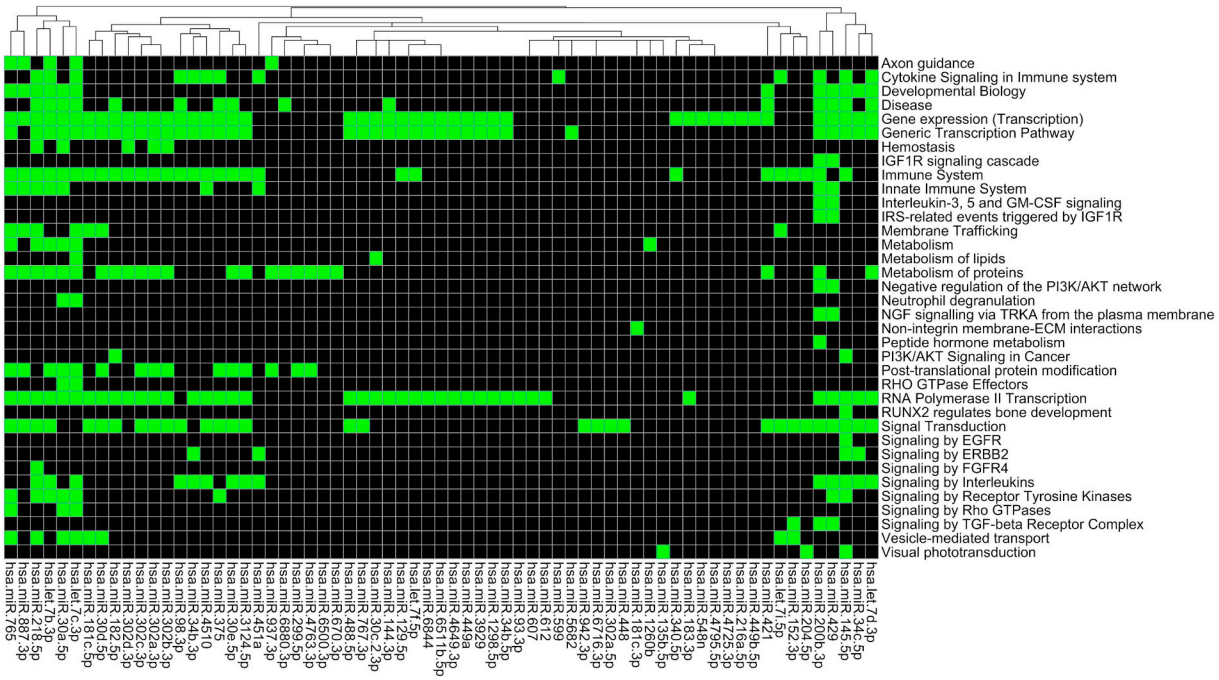

Fig. 3. Integration of differentially expressed miRNAs with enriched pathways. Integration of differentially expressed miRNAs with enriched pathways. Green segments represent an enriched pathway that was enriched for validated miRNA targets (Fisher exact test, adjusted p-value < .05). (For interpretation of the references to colour in this figure legend, the reader is referred to the web version of this article.)

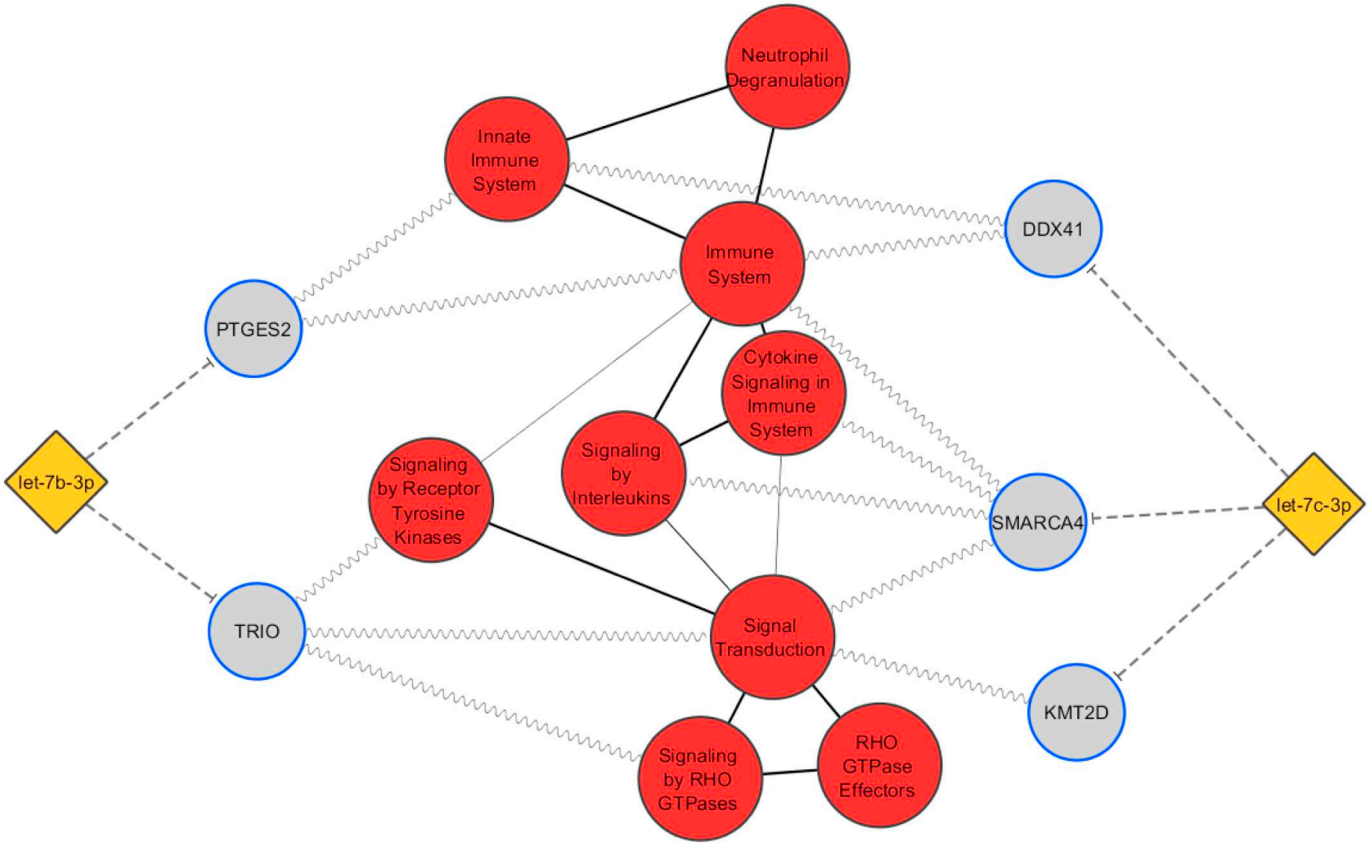

Fig. 4. Proposed interactions of miRNAs let-7b-5p and let-7c-5p with validated genes targets that are involved in inflammatory pathways. Yellow nodes represent miRNAs, grey nodes represent genes, red nodes represent pathways. The blue outline of the gene nodes indicates down-regulation of the gene. Edges between miRNAs and gene nodes indicates predicated target that was strongly negatively correlated with miRNA expression (Spearman's rank correlation < −0.7, adjusted p-value < .05). Edges between gene nodes and pathway nodes indicate that the gene is a member of that enriched pathway. Edges between pathway nodes indicates common genes in each pathway. (For interpretation of the references to colour in this figure legend, the reader is referred to the web version of this article.)

neuronal differentiation (Zhao et al., 2010). Let-7b has also been shown to interact with the long non-coding RNA H19 (Han et al., 2018b). Inhibition of let-7b via H19 contributes to apoptosis of hippocampal neurons in a rat model of MTLE (Han et al., 2018a). The function and expression of let-7c in the epileptogenic brain is less well studied. Overexpression of let-7c in human stem cells leads to morphological as well as functional deficits including impaired neuronal morphologic development, synapse formation and synaptic strength, as well as a marked reduction of neuronal excitability (McGowan et al., 2018). In one study let-7c expression did not change in the hippocampus of MTLE patients and in the cortex of FCD patients when compared to controls (Srivastava et al., 2017). However, in another study let-7c was found to be increased in serum of drug-responsive MTLE patients compared to drug-resistant MTLE patients (Wang et al., 2015). Both let-7b-3p and let-7c-3p remain interesting targets for further investigation in their role of regulation of the MTLE transcriptional network and whether they possess disease modifying properties.

Based on alterations to the mRNA transcriptome profile five compounds were identified that could counteract the gene expression changes identified in MTLE-HS: the MEK inhibitor PD-032590, the mTOR inhibitor deforolimus, the anti-inflammatory celastrol, the estrogen receptor agonist diarylpropionitrile, and dictamnine. Hyper-activation of the mTOR pathway is implicated in the pathogenesis of epilepsy associated with MTLE, tuberous sclerosis complex, cortical dysplasia and some genetic epilepsies (e.g., DEPDC5) (Crino, 2015; Wong, 2013). Since the mTOR and MEK pathways are interconnected, hyper-activation in MEK may also facilitate epileptogenesis and seizures (Conciatori et al., 2018). The mTOR pathway is suggested to be an anti-epileptogenic target (Galanopoulou et al., 2012), and the mTOR inhibitor everolimus is currently used in the clinic as adjunctive therapy for patients with tuberous sclerosis complex (Franz et al., 2018; French et al., 2016). The role of inflammation in a spectrum of experimental and human epilepsies is well established and several neuroinflammatory pathways have been identified as novel treatment targets for *epi*lepsy (van Vliet et al., 2018). The effects of estrogens on seizures is less clear (Velíšková et al., 2010). For decades, estrogens were considered proconvulsant, however, recent studies show that estrogens can be either excitatory or inhibitory. The estrogen receptor agonist diarylpropionitrile had anti-seizure effects in the pentylenetetrazole-induced seizures (Frye et al., 2009). However, estrogen can be proconvulsant in animals and humans (Scharfman and MacLusky, 2006). Finally, dictamnine is a furoquinoline antibiotic for which little is known about its potential central nervous system effects; however, it inhibits lipopolysaccharide-induced nitric oxide production in vitro and may have anti-oxidant and anti-inflammatory effects in the brain (Yoon et al., 2012). While this approach has previously been used to identify potential drug candidates for the treatment of cancer of which many have been validated in vitro (Musa et al., 2018), whether these compounds could be disease modifying for individuals with refractory *epi*lepsy requires further investigation.

A potential limitation of the presented study was the use of post-mortem brain tissue for the controls versus surgical resected material for the MTLE cases. Due to technical and ethical issues the use of post-mortem tissue as controls is standard practice in many human brain transcriptome studies. The general assumption is that sourcing RNA from brain tissue from two fundamentally different biological stages would result in the identification of transcriptional changes that reflect these stages rather than the disease of interest. Interestingly, the results presented here (Fig. 2b) suggest that this issue may be overstated. Indeed, when post-mortem brain tissue of the cortex was compared to surgical resected material from the cortex, only two differentially expressed genes were identified. Further, clustering of the transcriptional profiles of both tissue sources revealed that the profiles were similar. These results are in-line with what is known about the pathology of the cortex in MTLE. While, this study provides preliminary evidence that there are only minor transcriptional alterations when post-mortem brain tissue is compared to surgical tissue a more comprehensive and systematic study is required that analyses different RNA species, such as non-coding RNAs, across different brain regions. However, this result does suggest that the alterations in the small RNA profiles of the MTLE-ctx are likely to be disease related. It also must be noted that the MTLE material used for this study was taken from individuals who had been experiencing seizures for multiple years (range: 7–52 years), further no information on time since last seizure prior to operation was available, this makes it difficult delineate and attribute the identified transcriptional changes to underlying epileptogenic changes or as a consequence of seizure activity. Subsequent in vivo studies or in vitro studies would be required to elucidate which of the identified transcriptional changes can be attributed to epileptogenic events or as a symptom of seizure activity, and to further assess if any of the novel changes identified here could be utilized as a molecular target for treatment of MTLE. Finally, among the samples chosen for this study there was a selection bias towards male samples, this was due to the genders of the available of samples. This potential confounder was considered; however, clustering of samples showed no difference in the overall RNA-Seq and small RNA-Seq transcriptome profile between the female and male samples and as such any differences introduced by gender were considered minimal.

5. Conclusions

This study constitutes the most systematic transcriptomic analysis of MTLE brain tissue to date, by analyzing both the expression profiles of RNA and small RNA in parallel we provide new insights in MTLE pathogenesis. The transcriptome profile generated from RNA-Seq confirmed key pathogenic pathways activated, along with neuronal loss and activation of astrocytes and microglia in the hippocampus of MTLE patients. Through the integration of both RNA-Seq and small RNA-Seq the miRNAs let-7b-3p and let-7c-3p were identified as potential key regulators of multiple pathways related to MTLE pathology. Most interestingly, this study has identified a potential key role for other small non-coding RNA species, such as small nucleolar RNAs and small nuclear RNAs, in the pathogenesis of MTLE. These understudied elements of the transcriptome have emerging roles in other diseases, including cancer and Alzheimer's disease, but are yet to receive such attention in MTLE and related pathologies.

Supplementary data to this article can be found online at https://doi.org/10.1016/j.nbd.2019.104612.

Author contributions

OD, EA and JDM conceived and designed the study. JCB, RT, SI, JJA, MT, EA, OD, CS, BD contributed to the acquisition of the tissue samples and/or clinical data. JDM performed the bioinformatics analysis, with the support of BJC and MJ. All wet-laboratory experiments were performed by JDM, EAvV and JJA. JDM, EAvV, DF, SD, EA, and OD helped with data interpretation and the writing of the manuscript. All authors read, revised and approved the final manuscript.

Author statement

None of the material presented in this article has been published or is under consideration for publication elsewhere, including the internet.

Data availability

The datasets generated during and/or analyzed during the current study are available at the following repositories:

Primary

RNA-seq and small RNA-Seq data from MTLE and control patients: Sequence data has been deposited at the European Genome-phenome Archive (EGA), which is hosted by the EBI and the CRG, under the accession number: EGAS00001003922.

Further information about EGA can be found on https://ega-archive.org "The European Genome-phenome Archive of human data consented for biomedical research"(http://www.nature.com/ng/journal/v47/n7/full/ng.3312.html).

Secondary

Single cell RNA-seq data: NCBI's Gene Expression Omnibus (GEO). Accession Number: GSE67835.

Web link: www.ncbi.nlm.nih.gov/geo/query/acc.cgi?acc=GSE67835).

Declaration of Competing Interest

The authors declare no competing interests.

Acknowledgments

The research leading to these results has received funding from the NINDS UO1 NS090415 05 Center for SUDEP Research: The Neuropathology of SUDEP, Finding A Cure for Epilepsy and Seizures (FACES), European Union's Seventh Framework Program (FP7/2007-2013) under grant agreement 602102 (EPITARGET; EAvV, EA) and the Top Sector Life Sciences & Health via a PPP Allowance made available to the Dutch Epilepsy Foundation to stimulate public-private partnerships (EAvV, EA).

References

Bai, B., Wu, H., Street, C., Hanfelt, J., Cheng, D., Jin, P., Lah, J.J., Chen, P.-C., Montine, T.J., Peng, J., Mufson, E.J., Wang, X., Duong, D.M., Li, Y., Sun, Y.E., Hales, C.M., Wu, Z., Wingo, T.S., Bennett, D.A., Lin, L., Willcock, D.M., Levey, A., Szulwach, K.E., Diner, I., Xia, Q., Dammer, E.B., Gozal, Y., Rees, H.D., Jones, D.R., Fritz, J.J., Cantero, G., Gearing, M., Seyfried, N.T., Heilman, C.J., 2013. U1 small nuclear ribonucleoprotein complex and RNA splicing alterations in Alzheimer's disease. Proc. Natl. Acad. Sci. https://doi.org/10.1073/pnas.1310249110.

Bell, B., Lin, J.J., Seidenberg, M., Hermann, B., 2011. The neurobiology of cognitive disorders in temporal lobe epilepsy. Nat. Rev. Neurol. 7, 154–164. https://doi.org/10.1038/nrneurol.2011.3.

Blümcke, I., Thom, M., Aronica, E., Armstrong, D.D., Bartolomei, F., Bernasconi, A., Bernasconi, N., Bien, C.G., Cendes, F., Coras, R., Cross, J.H., Jacques, T.S., Kahane, P., Mathern, G.W., Miyata, H., Moshé, S.L., Oz, B., Özkara, Ç., Perucca, E., Sisodiya, S., Wiebe, S., Spreafico, R., 2013. International consensus classification of hippocampal sclerosis in temporal lobe epilepsy: a task force report from the ILAE commission on diagnostic methods. Epilepsia 54, 1315–1329. https://doi.org/10.1111/epi.12220.

Blumcke, I., Spreafico, R., Haaker, G., Coras, R., Kobow, K., Bien, C.G., Pfäfflin, M., Elger, C., Widman, G., Schramm, J., Becker, A., Braun, K.P., Leijten, F., Baayen, J.C., Aronica, E., Chassoux, F., Hamer, H., Stefan, H., Rössler, K., Thom, M., Walker, M.C., Sisodiya, S.M., Duncan, J.S., McEvoy, A.W., Pieper, T., Holthausen, H., Kudernatsch, M., Meencke, H.J., Kahane, P., Schulze-Bonhage, A., Zentner, J., Heiland, D.H., Urbach, H., Steinhoff, B.J., Bast, T., Tassi, L., Lo Russo, G., Özkara, C., Oz, B., Krsek, P., Vogelgesang, S., Runge, U., Lerche, H., Weber, Y., Honavar, M., Pimentel, J., Arzimanoglou, A., Ulate-Campos, A., Noachtar, S., Hartl, E., Schijns, O., Guerrini, R., Barba, C., Jacques, T.S., Cross, J.H., Feucht, M., Mühlebner, A., Grunwald, T., Trinka, E., Winkler, P.A., Gil-Nagel, A., Toledano Delgado, R., Mayer, T., Lutz, M., Zountsas, B., Garganis, K., Rosenow, F., Hermsen, A., von Oertzen, T.J., Diepgen, T.L., Avanzini, G., 2017. Histopathological findings in brain tissue obtained during epilepsy surgery. N. Engl. J. Med. https://doi.org/10.1056/nejmoa1703784.

Bolger, A.M., Lohse, M., Usadel, B., 2014. Trimmomatic: a flexible trimmer for Illumina sequence data. Bioinformatics 30, 2114–2120. https://doi.org/10.1093/bioinformatics/btu170.

Conciatori, F., Ciuffreda, L., Bazzichetto, C., Falcone, I., Pilotto, S., Bria, E., Cognetti, F., Milella, M., 2018. MTOR cross-talk in cancer and potential for combination therapy. Cancers (Basel). https://doi.org/10.3390/cancers10010023.

Crino, P.B., 2015. mTOR signaling in epilepsy: insights from malformations of cortical development. Cold Spring Harb. Perspect. Med. https://doi.org/10.1101/cshperspect.a022442.

Croft, D., O'Kelly, G., Wu, G., Haw, R., Gillespie, M., Matthews, L., Caudy, M., Garapati, P., Gopinath, G., Jassal, B., Jupe, S., Kalatskaya, I., MayMahajan, S., May, B., Ndegwa, N., Schmidt, E., Shamovsky, V., Yung, C., Birney, E., Hermjakob, H., D'Eustachio, P., Stein, L., 2011. Reactome: a database of reactions, pathways and biological processes. Nucleic Acids Res. 39. https://doi.org/10.1093/nar/gkq1018.

Darmanis, S., Sloan, S.A., Zhang, Y., Enge, M., Caneda, C., Shuer, L.M., Hayden Gephart, M.G., Barres, B.A., Quake, S.R., 2015. A survey of human brain transcriptome diversity at the single cell level. Proc. Natl. Acad. Sci. https://doi.org/10.1073/pnas.1507125112.

Devinsky, O., Spruill, T., Thurman, D., Friedman, D., 2016. Recognizing and preventing epilepsy-related mortality. Neurology 86, 779–786. https://doi.org/10.1212/WNL.0000000000002253.

Dixit, A.B., Banerjee, J., Srivastava, A., Tripathi, M., Sarkar, C., Kakkar, A., Jain, M., Chandra, P.S., 2016. RNA-seq analysis of hippocampal tissues reveals novel candidate genes for drug refractory epilepsy in patients with MTLE-HS. Genomics 107, 178–188. https://doi.org/10.1016/j.ygeno.2016.04.001.

Dredla, B.K., Lucas, J.A., Wharen, R.E., Tatum, W.O., 2016. Neurocognitive outcome following stereotactic laser ablation in two patients with MRI-/PET + mTLE. Epilepsy Behav. 56, 44–47. https://doi.org/10.1016/j.yebeh.2015.12.047.

Dweep, H., Gretz, N., 2015. miRWalk2.0: a comprehensive atlas of microRNA-target interactions. Nat. Methods 12, 697. https://doi.org/10.1038/nmeth.3485.

Dweep, H., Sticht, C., Pandey, P., Gretz, N., 2011. MiRWalk - database: prediction of possible miRNA binding sites by " walking" the genes of three genomes. J. Biomed. Inform. 44, 839–847. https://doi.org/10.1016/j.jbi.2011.05.002.

Engel, J., McDermott, M.P., Wiebe, S., Langfitt, J.T., Stern, J.M., Dewar, S., Sperling, M.R., Gardiner, I., Erba, G., Fried, I., Jacobs, M., Vinters, H.V., Mintzer, S., Kieburtz, K., 2012. Early surgical therapy for drug-resistant temporal lobe epilepsy: a randomized trial. JAMA - J. Am. Med. Assoc. 307, 922–930. https://doi.org/10.1001/jama.2012.220.

Fabregat, A., Jupe, S., Matthews, L., Sidiropoulos, K., Gillespie, M., Garapati, P., Haw, R., Jassal, B., Korninger, F., May, B., Milacic, M., Roca, C.D., Rothfels, K., Sevilla, C., Shamovsky, V., Shorser, S., Varusai, T., Viteri, G., Weiser, J., Wu, G., Stein, L., Hermjakob, H., D'Eustachio, P., 2018. The Reactome pathway knowledgebase. Nucleic Acids Res. 46, D649–D655. https://doi.org/10.1093/nar/gkx1132.

Franz, D.N., Lawson, J.A., Yapici, Z., Brandt, C., Kohrman, M.H., Wong, M., Milh, M., Wiemer-Kruel, A., Voi, M., Coello, N., Cheung, W., Grosch, K., French, J.A., 2018. Everolimus dosing recommendations for tuberous sclerosis complex–associated refractory seizures. Epilepsia. https://doi.org/10.1111/epi.14085.

French, J.A., Lawson, J.A., Yapici, Z., Ikeda, H., Polster, T., Nabbout, R., Curatolo, P., de Vries, P.J., Dlugos, D.J., Berkowitz, N., Voi, M., Peyrard, S., Pelov, D., Franz, D.N., 2016. Adjunctive everolimus therapy for treatment-resistant focal-onset seizures associated with tuberous sclerosis (EXIST-3): a phase 3, randomised, double-blind, placebo-controlled study. Lancet.(16). https://doi.org/10.1016/S0140-6736.31419–2.

Frye, C.A., Ryan, A., Rhodes, M., 2009. Antiseizure effects of 3α-androstanediol and/or 17β-estradiol may involve actions at estrogen receptor β. Epilepsy Behav. 16, 418–422. https://doi.org/10.1016/j.yebeh.2009.09.008.

Galanopoulou, A.S., Gorter, J.A., Cepeda, C., 2012. Finding a better drug for epilepsy: the mTOR pathway as an antiepileptogenic target. Epilepsia. https://doi.org/10.1111/j.1528-1167.2012.03506.x.

Griffin, N.G., Wang, Y., Hulette, C.M., Halvorsen, M., Cronin, K.D., Walley, N.M., Haglund, M.M., Radtke, R.A., Skene, J.H.P., Sinha, S.R., Heinzen, E.L., 2016. Differential gene expression in dentate granule cells in mesial temporal lobe epilepsy with and without hippocampal sclerosis. Epilepsia. https://doi.org/10.1111/epi.13305.

Griffiths-Jones, S., Saini, H.K., van Dongen, S., Enright, A.J., 2008. miRBase: tools for microRNA genomics. Nucleic Acids Res. 36, D154–D158. https://doi.org/10.1093/nar/gkm952.

Han, C.L., Ge, M., Liu, Y.P., Zhao, X.M., Wang, K.L., Chen, N., Hu, W., Zhang, J.G., Li, L., Meng, F.G., 2018a. Long non-coding RNA H19 contributes to apoptosis of hippocampal neurons by inhibiting let-7b in a rat model of temporal lobe epilepsy. Cell Death Dis. 9, 617. https://doi.org/10.1038/s41419-018-0496-y.

Han, C.L., Ge, M., Liu, Y.P., Zhao, X.M., Wang, K.L., Chen, N., Meng, W.J., Hu, W., Zhang, J.G., Li, L., Meng, F.G., 2018b. LncRNA H19 contributes to hippocampal glial cell activation via JAK/STAT signaling in a rat model of temporal lobe epilepsy. J. Neuroinflammation. https://doi.org/10.1186/s12974-018-1139-z.

Harrow, J., Frankish, A., Gonzalez, J.M., Tapanari, E., Diekhans, M., Kokocinski, F., Aken, B.L., Barrell, D., Zadissa, A., Searle, S., Barnes, I., Bignell, A., Boychenko, V., Hunt, T., Kay, M., Mukherjee, G., Rajan, J., Despacio-Reyes, G., Saunders, G., Steward, C., Harte, R., Lin, M., Howald, C., Tanzer, A., Derrien, T., Chrast, J., Walters, N., Balasubramanian, S., Pei, B., Tress, M., Rodriguez, J.M., Ezkurdia, I., Van Baren, J., Brent, M., Haussler, D., Kellis, M., Valencia, A., Reymond, A., Gerstein, M., Guigó, R., Hubbard, T.J., 2012. GENCODE: the reference human genome annotation for the ENCODE project. Genome Res. 22, 1760–1774. https://doi.org/10.1101/gr.135350.111.

Kaalund, S.S., Venø, M.T., Bak, M., Møller, R.S., Laursen, H., Madsen, F., Broholm, H., Quistorff, B., Uldall, P., Tommerup, N., Kauppinen, S., Sabers, A., Fluiter, K., Møller, L.B., Nossent, A.Y., Silahtaroglu, A., Kjems, J., Aronica, E., Tümer, Z., 2014. Aberrant expression of miR-218 and miR-204 in human mesial temporal lobe epilepsy and hippocampal sclerosis-convergence on axonal guidance. Epilepsia 55, 2017–2027. https://doi.org/10.1111/epi.12839.

Kang, J.Y., Wu, C., Tracy, J., Lorenzo, M., Evans, J., Nei, M., Skidmore, C., Mintzer, S., Sharan, A.D., Sperling, M.R., 2016. Laser interstitial thermal therapy for medically intractable mesial temporal lobe epilepsy. Epilepsia 57, 325–334. https://doi.org/10.1111/epi.13284.

Kim, D., Pertea, G., Trapnell, C., Pimentel, H., Kelley, R., Salzberg, S.L., 2013. TopHat2: accurate alignment of transcriptomes in the presence of insertions, deletions and gene fusions. Genome Biol. 14, R36. https://doi.org/10.1186/gb-2013-14-4-r36.

Korotkov, A., Mills, J.D., Gorter, J.A., van Vliet, E.A., Aronica, E., 2017. Systematic review and meta-analysis of differentially expressed miRNAs in experimental and human temporal lobe epilepsy. Sci. Rep. https://doi.org/10.1038/s41598-017-11510-8.

Kozomara, A., Griffiths-Jones, S., 2014. MiRBase: annotating high confidence microRNAs using deep sequencing data. Nucleic Acids Res. 42. https://doi.org/10.1093/nar/gkt1181.

Langmead, B., Salzberg, S.L., 2012. Fast gapped-read alignment with bowtie 2. Nat. Methods 9, 357–359. https://doi.org/10.1038/nmeth.1923.

Lee, H., Han, S., Kwon, C.S., Lee, D., 2016. Biogenesis and regulation of the let-7 miRNAs

and their functional implications. Protein Cell. https://doi.org/10.1007/s13238-015-0212-y.

Liao, J., Yu, L., Mei, Y., Guarnera, M., Shen, J., Li, R., Liu, Z., Jiang, F., 2010. Small nucleolar RNA signatures as biomarkers for non-small-cell lung cancer. Mol. Cancer. https://doi.org/10.1186/1476-4598-9-198.

Liao, Y., Smyth, G.K., Shi, W., 2014. FeatureCounts: an efficient general purpose program for assigning sequence reads to genomic features. Bioinformatics 30, 923–930. https://doi.org/10.1093/bioinformatics/btt656.

Love, M.I., Huber, W., Anders, S., 2014. Moderated estimation of fold change and dispersion for RNA-seq data with DESeq2. Genome Biol. 15, 550. https://doi.org/10.1186/s13059-014-0550-8.

McGowan, H., Mirabella, V.R., Hamod, A., Karakhanyan, A., Mlynaryk, N., Moore, J.C., Tischfield, J.A., Hart, R.P., Pang, Z.P., 2018. hsa-let-7c miRNA regulates synaptic and neuronal function in human neurons. Front. Synaptic Neurosci. 10, 19. https://doi.org/10.3389/fnsyn.2018.00019.

Mei, Y.P., Liao, J.P., Shen, J., Yu, L., Liu, B.L., Liu, L., Li, R.Y., Ji, L., Dorsey, S.G., Jiang, Z.R., Katz, R.L., Wang, J.Y., Jiang, F., 2012. Small nucleolar RNA 42 acts as an oncogene in lung tumorigenesis. Oncogene. https://doi.org/10.1038/onc.2011.449.

Mills, J.D., Iyer, A.M., Van Scheppingen, J., Bongaarts, A., Anink, J.J., Janssen, B., Zimmer, T.S., Spliet, W.G., Van Rijen, P.C., Jansen, F.E., Feucht, M., Hainfellner, J.A., Krsek, P., Zamecnik, J., Kotulska, K., Jozwiak, S., Jansen, A., Lagae, L., Curatolo, P., Kwiatkowski, D.J., Jeroen Pasterkamp, R., Senthilkumar, K., Von Oerthel, L., Hoekman, M.F., Gorter, J.A., Crino, P.B., Mühlebner, A., Scicluna, B.P., Aronica, E., 2017. Coding and small non-coding transcriptional landscape of tuberous sclerosis complex cortical tubers: implications for pathophysiology and treatment. Sci. Rep. 7. https://doi.org/10.1038/s41598-017-06145-8.

Musa, A., Ghoraie, L.S., Zhang, S.D., Glazko, G., Yli-Harja, O., Dehmer, M., Haibe-Kains, B., Emmert-Streib, F., 2018. A review of connectivity map and computational approaches in pharmacogenomics. Brief. Bioinform. https://doi.org/10.1093/bib/bbw112.

Pruitt, R., Gamble, A., Black, K., Schulder, M., Mehta, A.D., 2016. Complication avoidance in laser interstitial thermal therapy: lessons learned. J. Neurosurg. 126, 1238–1245. https://doi.org/10.3171/2016.3.jns152147.

Scharfman, H.E., MacLusky, N.J., 2006. The influence of gonadal hormones on neuronal excitability, seizures, and epilepsy in the female. Epilepsia. https://doi.org/10.1111/j.1528-1167.2006.00672.x.

Shannon, P., Markiel, A., Ozier, O., Baliga, N.S., Wang, J.T., Ramage, D., Amin, N., Schwikowski, B., Ideker, T., 2003. Cytoscape: a software environment for integrated models of biomolecular interaction networks. Genome Res. 13, 2498–2504. https://doi.org/10.1101/gr.1239303.

Srivastava, A., Dixit, A.B., Paul, D., Tripathi, M., Sarkar, C., Chandra, P.S., Banerjee, J., 2017. Comparative analysis of cytokine/chemokine regulatory networks in patients with hippocampal sclerosis (HS) and focal cortical dysplasia (FCD). Sci. Rep. 7, 15904. https://doi.org/10.1038/s41598-017-16041-w.

Subramanian, A., Narayan, R., Corsello, S.M., Peck, D.D., Natoli, T.E., Lu, X., Gould, J., Davis, J.F., Tubelli, A.A., Asiedu, J.K., Lahr, D.L., Hirschman, J.E., Liu, Z., Donahue, M., Julian, B., Khan, M., Wadden, D., Smith, I.C., Lam, D., Liberzon, A., Toder, C., Bagul, M., Orzechowski, M., Enache, O.M., Piccioni, F., Johnson, S.A., Lyons, N.J., Berger, A.H., Shamji, A.F., Brooks, A.N., Vrcic, A., Flynn, C., Rosains, J., Takeda, D.Y., Hu, R., Davison, D., Lamb, J., Ardlie, K., Hogstrom, L., Greenside, P., Gray, N.S., Clemons, P.A., Silver, S., Wu, Xiaoyun, Zhao, W.-N., Read-Button, W., Wu, Xiaohua, Haggarty, S.J., Ronco, L.V., Boehm, J.S., Schreiber, S.L., Doench, J.G., Bittker, J.A., Root, D.E., Wong, B., Golub, T.R., 2017. A next generation connectivity map: L1000 platform and the first 1,000,000 profiles. Cell 171, 1437–1452.e17. https://doi.org/10.1016/j.cell.2017.10.049.

Thom, M., 2004. Recent advances in the neuropathology of focal lesions in epilepsy. Expert. Rev. Neurother. https://doi.org/10.1586/14737175.4.6.973.

Väremo, L., Nielsen, J., Nookaew, I., 2013. Enriching the gene set analysis of genome-wide data by incorporating directionality of gene expression and combining statistical hypotheses and methods. Nucleic Acids Res. 41, 4378–4391. https://doi.org/10.1093/nar/gkt111.

Velíšková, J., De Jesus, G., Kaur, R., Velíšek, L., 2010. Females, their estrogens, and seizures. Epilepsia. https://doi.org/10.1111/j.1528-1167.2010.02629.x.

van Vliet, E.A., Aronica, E., Vezzani, A., Ravizza, T., 2018. Review: Neuroinflammatory pathways as treatment targets and biomarker candidates in epilepsy: emerging evidence from preclinical and clinical studies. Neuropathol. Appl. Neurobiol. https://doi.org/10.1111/nan.12444.

Wang, J., Tan, Lan, Tan, Lin, Tian, Y., Ma, J., Tan, C.C., Wang, H.F., Liu, Y., Tan, M.S., Jiang, T., Yu, J.T., 2015. Circulating microRNAs are promising novel biomarkers for drug-resistant epilepsy. Sci. Rep. 5, 10201. https://doi.org/10.1038/srep10201.

Wong, M., 2013. A critical review of mTOR inhibitors and epilepsy: from basic science to clinical trials. Expert. Rev. Neurother. https://doi.org/10.1586/ern.13.48.

Yoon, J.S., Jeong, E.J., Yang, H., Kim, S.H., Sung, S.H., Kim, Y.C., 2012. Inhibitory alkaloids from Dictamnus dasycarpus root barks on lipopolysaccharide-induced nitric oxide production in BV2 cells. J. Enzyme Inhib. Med. Chem. https://doi.org/10.3109/14756366.2011.598151.

Zhao, C., Sun, G., Li, S., Lang, M.-F., Yang, S., Li, W., Shi, Y., 2010. MicroRNA let-7b regulates neural stem cell proliferation and differentiation by targeting nuclear receptor TLX signaling. Proc. Natl. Acad. Sci. 107, 1876–1881. https://doi.org/10.1073/pnas.0908750107.